Post-transcriptional Regulation of P-Glycoprotein Expression in Cancer Cell Lines

Angeles Gómez-Martínez,[1] Pilar García-Morales,[1] Alfredo Carrato,[1,2] María D. Castro-Galache,[1] José L. Soto,[2] Estefanía Carrasco-García,[1] Miriam García-Bautista,[2] Patricia Guaraz,[2] José A. Ferragut,[1] and Miguel Saceda[1,2]

[1]Instituto de Biología Molecular y Celular, Universidad Miguel Hernández and [2]Hospital Universitario Elche 03203 Elche (Alicante), Spain

Abstract

The present study of inhibitors shows that the histone deacetylase–induced increase in P-glycoprotein (Pgp) mRNA (MDR1 mRNA) does not parallel either an increase in Pgp protein or an increase in Pgp activity in several colon carcinoma cell lines. Furthermore, studying the polysome profile distribution, we show a translational control of Pgp in these cell lines. In addition, we show that the MDR1 mRNA produced in these cell lines is shorter in its 5′ end that the MDR1 mRNA produced in the MCF-7/Adr (human breast carcinoma) and K562/Adr (human erythroleukemia) cell lines, both of them expressing Pgp. The different size of the MDR1 mRNA is due to the use of alternative promoters. Our data suggest that the translational blockade of MDR1 mRNA in the colon carcinoma cell lines and in wild-type K562 cells could be overcome by alterations in the 5′ end of the MDR1 mRNA in the resistant variant of these cell lines, as in the case of the K562/Adr cell line. This is, to our knowledge, the first report demonstrating that the presence of an additional 5′ untranslated fragment in the MDR1 mRNA improves the translational efficiency of this mRNA.
(Mol Cancer Res 2007;5(6):641–53)

Introduction

Multidrug resistance (MDR) constitutes a major obstacle for the success of cancer treatment. The MDR phenotype is responsible for resistance to a wide variety of anticancer drugs, such as anthracyclines, *Vinca* alkaloids, and others (1). Although several mechanisms could be involved in the acquisition of this phenotype, the role of two different membrane proteins, P-glycoprotein (Pgp) and MDR-associated protein (MRP), has been well established (2-4). Both proteins are members of the same ATP-binding cassette superfamily of transport proteins. Pgp was first identified as a consequence of its overexpression in multidrug-resistant tumor cells, where it mediates the ATP-dependent efflux of a variety of chemotherapeutic agents. In addition to its role during the acquisition of the MDR phenotype, Pgp is expressed in normal tissues, both as a consequence of differentiation and also in response to environmental challenges, and it has been proposed to play a role as a cell protector against cellular toxins (5). In addition, a general antiapoptotic role for Pgp has been proposed (6). It is clear that Pgp shows several functions in different cells and tissues.

Pgp is encoded by a multigene family in higher eukaryotes (7). The *MDR1* gene encodes the human Pgp. In cultured cells, constitutive overexpression of Pgp is mediated by changes in gene dosage or transcription. Pgp can also be transiently induced in cultured cells by a variety of stimuli, such as heat shock, UV radiation, and chemotherapeutic agents (8-11). The regulation of Pgp expression has been mostly related to transcriptional control of the *mdr1* gene expression (8-11). The proximal promoter of mdr1 contains several regulatory regions, such as an inverted CCAAT box and a GC element, both of which are required for constitutive promoter activity in several cell lines (12-16). Recently, it has been reported that in the colon carcinoma cell line SW620, trichostatin A (TSA), a histone deacetylase inhibitor (iHDAC), induces an increase in *mdr1* transcription through the inverted CCAAT box element, with the requirement of the NF-Y transcription factor (17). This result can represent a big problem because a number of iHDACs are able to inhibit tumor growth, and several of them are used in clinical trials (18); however, an increase in Pgp expression mediated by these compounds would make their combination with other cytotoxic agents that are substrates of Pgp impossible. We have investigated in the human colon carcinoma cell lines SW620, HT-29, and HT-29/M6 the effect of the iHDACs TSA and suberoylanilide hydroxamic acid (SAHA) on Pgp expression, demonstrating a translational control of Pgp. The MDR1 mRNA produced in these cell lines is 285 bp shorter that the MDR1 mRNA produced in the human MCF-7/Adr and K562/Adr cell lines, both of them expressing Pgp protein. The different size of the MDR1 mRNA is due to the use of alternative promoters. This is, to our knowledge, the first work demonstrating that the presence of a 285-bp additional 5′ untranslated fragment in the MDR1 mRNA improves the translational efficiency of this mRNA.

Received 6/26/06; revised 3/7/07; accepted 3/19/07.
Grant support: Instituto de Salud Carlos III Grants FIS 04/1000 and FIS 05/0969.
The costs of publication of this article were defrayed in part by the payment of page charges. This article must therefore be hereby marked *advertisement* in accordance with 18 U.S.C. Section 1734 solely to indicate this fact.
Note: Supplementary data for this article are available at Molecular Cancer Research Online (http://mcr.aacrjournals.org/).
Requests for reprints: Miguel Saceda, Instituto de Biología Molecular y Celular, Ed. Torregaitan, Universidad Miguel Hernández, 03202 Elche (Alicante), Spain. Phone: 34-96-6658432; Fax: 34-96-6658758. E-mail: msaceda@umh.es

doi:10.1158/1541-7786.MCR-06-0177

Results

Effect of Histone Deacetylase Inhibitors on MDR1 mRNA in Different Colon Carcinoma Cell Lines

To determine whether the TSA-induced increase in MDR1 mRNA expression observed in the human colon carcinoma cell line SW620 (17) was a specific phenomenon related to a particular cell line or it constitutes a more general phenomenon, we have determined the level of MDR1 mRNA in SW620, HT-29, and HT-29/M6 human colon carcinoma cell lines in the presence and absence of TSA. Results in Fig. 1A show that TSA treatment induces an increase in MDR1 mRNA in the three cell lines. As internal control, we have used glyceraldehyde-3-phosphate dehydrogenase (GAPDH) mRNA.

Despite the increase in MDR1 mRNA levels, we observed that TSA and other iHDACs inhibited the cell growth in SW620, HT-29, and HT-29/M6 cells, as determined by crystal violet staining (data not shown). Furthermore, we found that independent of the observed increase in MDR1 mRNA, TSA and SAHA were able to induce apoptosis in these cell lines, as shown by the presence of a sub-G_1 peak determined by flow cytometry analysis after treatment with iHDACs (Fig. 1B and Supplementary Fig. S1). Apoptosis induction was also shown by FITC-Annexin V staining of the externalized phosphatidylserine (data not shown).

Effect of Histone Deacetylase Inhibitors on P-Glycoprotein Expression

To test whether the increase observed in the level of MDR1 mRNA does parallel an increase in Pgp protein, we analyzed Pgp protein levels in HT-29 and HT-29/M6 cells in the presence and in the absence of TSA by Western immunoblot using as a positive control the murine leukemia cell line L1210R that expresses high levels of Pgp protein (19). As shown in Fig. 2A, there is no evidence of Pgp protein expression in HT-29 and HT-29/M6 cells either in the presence or in the absence of TSA. We further confirm this observation by immunocytochemistry, and again, we did not find protein expression in the presence or absence of TSA (data not shown).

We also studied the activity of Pgp using two different experimental approaches. First, we analyzed the accumulation of daunomycin, a fluorescent substrate of Pgp, by flow cytometry in the presence and absence of iHDACs in L1210R and K562/Adr cells. The presence of an active Pgp in these cell lines was shown by the increased accumulation of daunomycin after verapamil (a Pgp inhibitor) addition (Supplementary Fig. S2). Results in Fig. 2B show that no functional Pgp was present in SW620, HT-29, and HT-29/M6 cells, either in the presence or in the absence of TSA. Second, we did a calcein assay in the presence and in the absence of verapamil. Results in Fig. 2C show the absence of an active Pgp in HT-29 and HT-29/M6 cells despite the increase observed in MDR1 mRNA expression.

Subcellular Distribution of MDR1 mRNA and Translational Control of MDR1 mRNA

Because the increase in MDR1 mRNA after iHDACs treatment did not parallel an increase in Pgp protein expression or activity, we analyzed by real-time reverse transcription-PCR (RT-PCR) the subcellular distribution of MDR1 mRNA. Nuclear and cytoplasmic RNA were extracted from HT-29 and HT-29/M6 cells treated or not with TSA. As a control, nuclear and cytoplasmic RNA from the Pgp-expressing MCF-7/Adr cell line was also extracted (20-22). In Fig. 3A, the same proportion of the nuclear and cytoplasmic extracts was

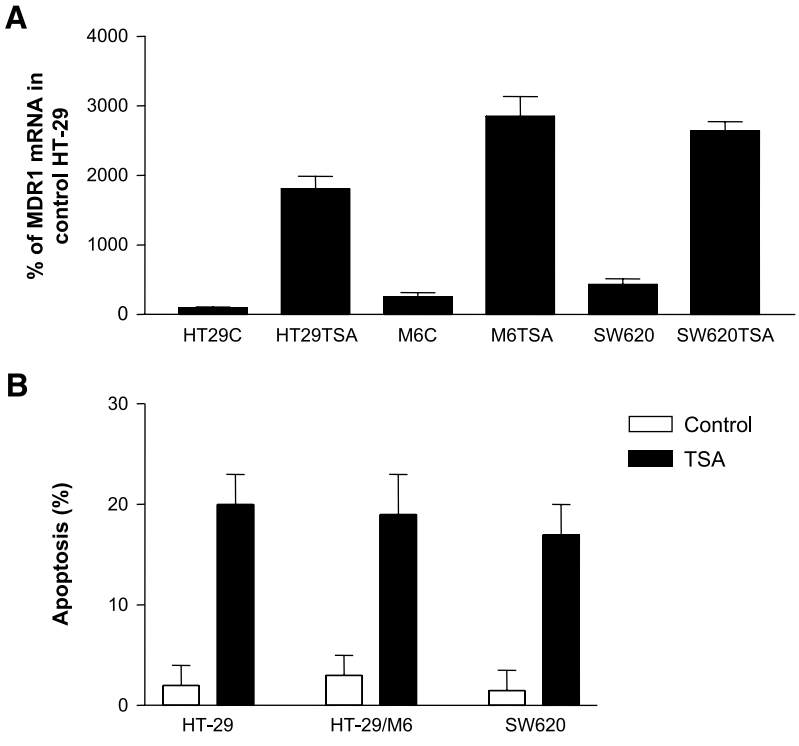

FIGURE 1. A. Analysis by real-time PCR of MDR1 mRNA in colon cancer cells. HT-29, HT-29/M6, and SW620 cell lines were treated or not with 0.5 μmol/L TSA for 24 h. As internal control, GAPDH mRNA was also determined, and MDR1 mRNA levels were normalized to GAPDH mRNA levels. Columns, means of at least three independent experiments with three replicates in each experiment; bars, SD. **B.** TSA effect on apoptosis induction in colon cancer cells. TSA-induced apoptosis in colon carcinoma cell lines determined as the percentage of cells in the sub-G_1 phase. HT-29, HT-29/M6, and SW620 cell lines were treated or not with 0.5 μmol/L TSA for 24 h, and cell cycle distribution was analyzed by flow cytometry as described in Materials and Methods. Columns, means of at least three independent experiments; bars, SD.

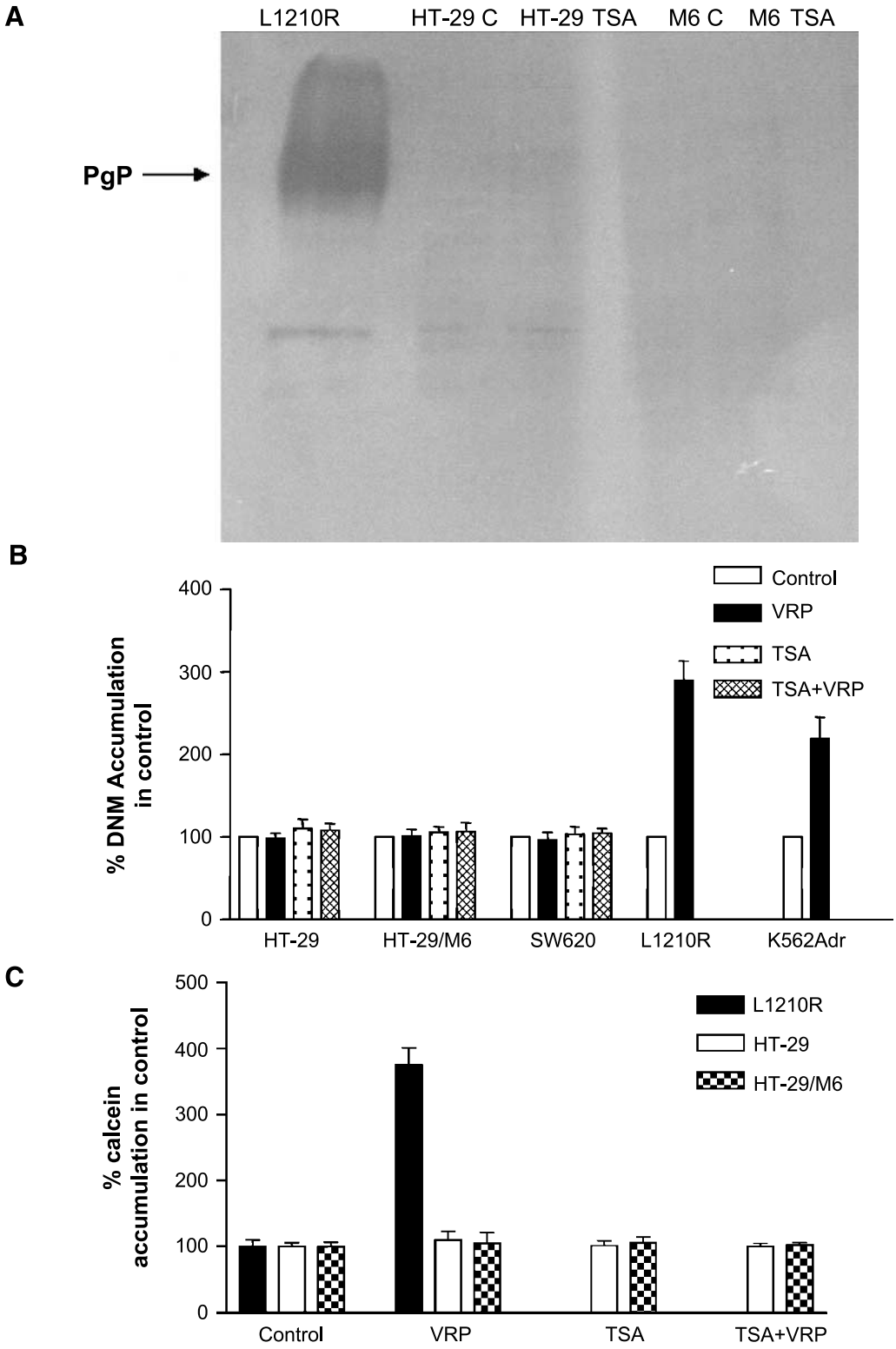

FIGURE 2. Determination of Pgp protein expression and activity in colon cancer cells. **A.** Western blot analysis of Pgp expression in HT-29 and HT-29/M6 colon carcinoma cell lines treated or not with 0.5 μmol/L TSA for 24 h. The Pgp-expressing L1210R murine leukemia cell line is included as a positive control. **B.** Pgp activity in HT-29, HT-29/M6, and SW620 cells treated or not with 0.5 μmol/L TSA for 24 h and in the presence or absence of 2.5 μmol/L verapamil (*VRP*). Pgp activity was estimated as daunomycin accumulation determined by flow cytometry. Daunomycin accumulation with verapamil in L1210R and K562/Adr cells is included as positive control. **C.** Pgp activity in HT-29 and HT-29/M6 cells treated or not with 0.5 μmol/L TSA for 24 h and in the presence or absence of 2.5 μmol/L verapamil. Pgp activity was estimated by the intracellular content of fluorescent calcein. In **B** and **C**, columns, means of at least three independent experiments using triplicates in each experiment; bars, SD.

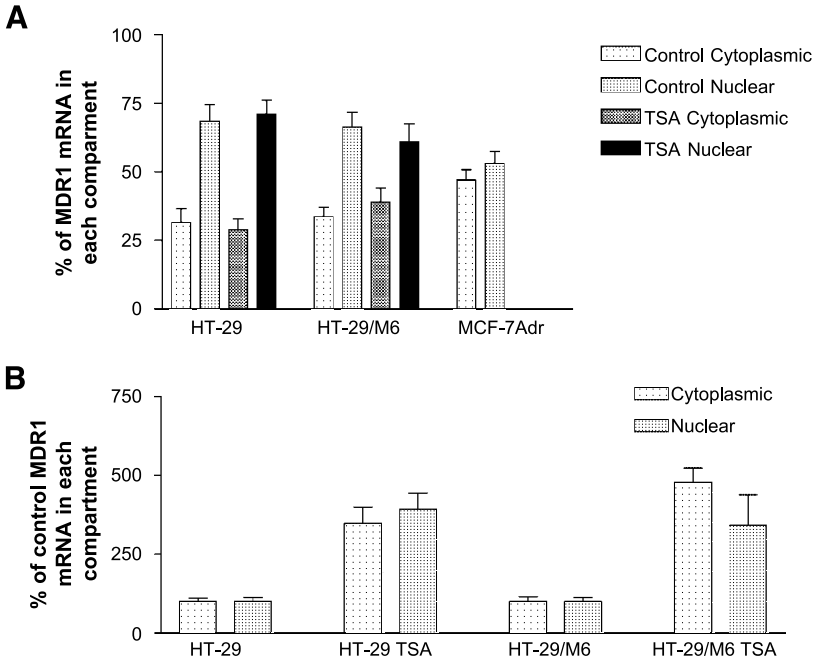

FIGURE 3. Subcellular distribution of MDR1 mRNA and GAPDH mRNA in colon cancer cells. **A.** Real-time RT-PCR analysis of MDR1 mRNA subcellular distribution in HT-29 and HT-29/M6 cells treated or not with 0.5 μmol/L TSA for 24 h. Equal proportions of the nuclear and cytoplasmic extracts were analyzed, and then each value is represented as the percentage of the sum of both. MDR1 mRNA values from MCF-7/Adr are included as a positive control. **B.** The results obtained in **A** are presented as the percentage of the MDR1 mRNA in each compartment in untreated cells. In **A** and **B**, columns, mean of at least three independent experiments; bars, SD.

evaluated and then expressed as the percentage of the sum of both fractions. Our results show that TSA did not modify significantly the percentage distribution of the MDR1 mRNA (nuclear versus cytoplasmic). However, as shown in Fig. 3B, when the MDR1 mRNA present in each compartment after TSA treatment was compared with the MDR1 mRNA present in untreated cells, TSA induced an increase in MDR1 mRNA levels in both compartments. Hence, the increase in MDR1 total mRNA levels after TSA treatment corresponds to an increase in both cytoplasmic and nuclear MDR1 mRNAs in HT-29 and HT-29/M6 cells. Then, we wanted to analyze whether the mRNA from the cytoplasmic fraction after TSA treatment was able to interact with the ribosomal machinery to generate Pgp protein. First, we separated the free ribosomes from the membrane-bound ribosomes using a sucrose gradient, and then, we analyzed the presence of MDR1 mRNA in these fractions. We observed that as an average, 85 ± 7.7% (mean ± SD) of the MDR1 mRNA detected in all samples seemed associated with membrane-bound ribosomes, as expected for a protein with transmembrane regions that is expressed in the cytoplasmic membrane. TSA treatment produced an increase in MDR1 mRNA levels associated to membrane-bound ribosomes in HT-29 and HT-29/M6 cells of 255 ± 15% and 570 ± 68%, respectively.

However, despite this increase, no expression of Pgp protein could be found in these cell lines, suggesting a translational control of the Pgp expression. To study the regulation of this translational control, we determined whether the association of the MDR1 mRNA to the membrane-bound ribosomes rendered MDR1 mRNA associated to polysomes or, if on the contrary, the association between MDR1 mRNA and ribosomes was only at the level of monosomes. Polysome profiles were done, and results are shown in Fig. 4A, demonstrating a biphasic distribution of MDR1 mRNA with a main fraction of MDR1 mRNA associated to monosomes. However, a substantial percentage of the MDR1 mRNA was associated with the polysome fraction, suggesting that some MDR1 mRNA should be effectively translated. This MDR1 mRNA seemed associated to the same fractions as control mRNAs, such as Mucin-1 (Muc-1) and epidermal growth factor receptor (EGFR) mRNAs, that are translated in the colon carcinoma cell lines (Fig. 4B), suggesting again that these fractions represent translationally active polysomes. As a quality control for polysome and monosome peak localization, absorbance at 254 nm was determined in the different fractions (data not shown).

Because we were not able to find expression of Pgp protein in HT-29 and HT-29/M6 cells treated or not with TSA, we did polysome profiles for Pgp, Muc-1, and other control genes in the presence and absence of puromycin, which blocks protein translation, inducing premature release of the mRNAs associated to polysomes (22). Results in Fig. 5A and Supplementary Fig. S3 show that, as expected, puromycin treatment induced an increase in the Muc-1 and EGFR mRNAs associated with the monosome fractions (fractions 1 to 10 of polysome profile) and a parallel decrease of these mRNAs associated to the polysome fractions (fractions 11 to 20 of polysome profile). However, MDR1 mRNA distribution was not affected by puromycin treatment, suggesting that MDR1 mRNA is not translationally active despite its association with the polysome fraction.

To rule out the possibility that Pgp protein was not detected due to a rapid turnover of the protein, Western blot analysis was done in HT-29 and HT-29/M6 cells treated with different proteases and proteasome inhibitors because Pgp protein turnover induced by the proteasome activity has been previously reported (23). None of these treatments resulted in Pgp protein detection The results using proteasome inhibitors are shown in Fig. 5B. We have also tried the combination of TSA treatment and proteasome inhibitors; as shown in Fig. 5C, no Pgp expression was detected in such conditions.

Mapping of MDR1 mRNA in HT-29/M6 Cells

To compare MDR1 mRNA in HT-29/M6 cells versus MCF-7/Adr cells, we first tried to amplify the complete MDR1 mRNA by RT-PCR using the appropriate 5′ and 3′ primers. As shown in Fig. 6A, we were able to obtain the complete MDR1 cDNA using RNA from MCF-7/Adr cells. However, we were not able to obtain this cDNA using RNA from HT-29/M6 cells. Appropriate control amplifications showed that the lack of results in the HT-29/M6 cell line was not due to the degradation of the RNA.

To further characterize the differences between MDR1 mRNA in HT-29/M6 and MCF-7/Adr cells, internal primers were designed to amplify by RT-PCR the fragments corresponding to the 5′ and 3′ ends. As shown in Fig. 6B and C, we were able to obtain the cDNAs corresponding to the 3′ end of the MDR1 mRNA in both cell lines. However, the 5′ end of the mRNA was amplified in MCF-7/Adr but not in HT-29/M6, suggesting some differences between the MDR1 mRNA of these cell lines in the 5′ end of the mRNA (Fig. 6B). Similar results to those obtained with the HT-29/M6 cells were obtained when HT-29 and SW620 cell lines were analyzed with the same primers (data not shown).

To map more precisely these differences, we generated a set of primers covering all the 5′ end fragment of the MDR1 mRNA at 400-bp intervals. When the RNA from MCF-7/Adr, SW620, K562, and K562/Adr cell lines was analyzed by RT-PCR using this set of primers, we found that only the F1 primer covering the first 400 bp of the 5′ end was unable to amplify MDR1 mRNA from SW620 and K562 RNAs (Fig. 7A). However, the same primer was able to amplify MDR1 mRNA from MCF-7/Adr and K562/Adr RNAs. All the other primers were able to amplify MDR1 mRNA in MCF-7/Adr, SW620, K562, and K562/Adr cell lines (Fig. 7B), suggesting that the differences observed between the MCF-7/Adr and HT-29 MDR1 mRNAs lay on the first 400 bp of the MDR1 mRNA. The different 5′ untranslated region (UTR) sequences (long and short) and a splicing form of the long 5′UTR were determined and are submitted as Supplementary Fig. S4.

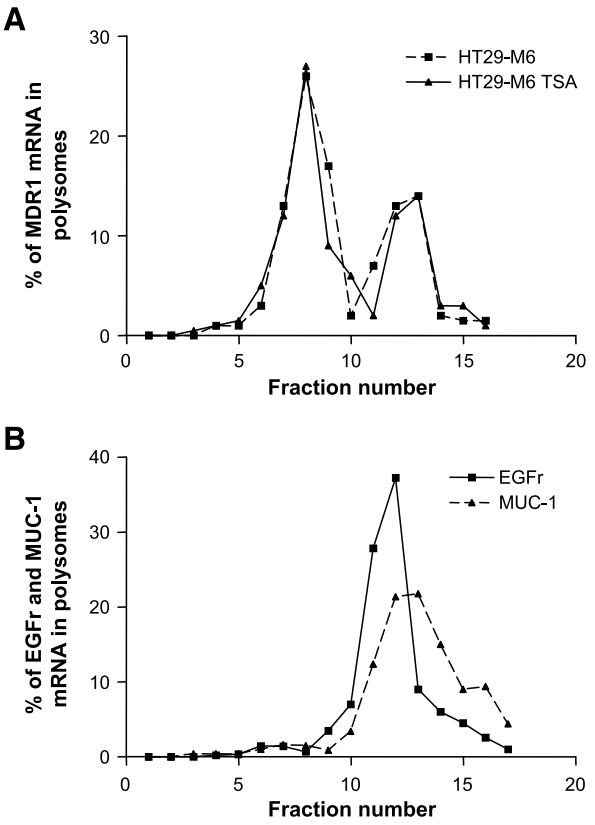

FIGURE 4. Polysome profile distribution of different mRNAs in the HT-29/M6 cell line. **A.** Polysome profile distribution of MDR1 mRNA in HT-29/M6 cells treated or not with TSA. **B.** Polysome profile distribution of EGFR and Muc-1 mRNAs in HT-29/M6 cells.

Role of the 5′ UTR of the MDR1 mRNA in Translational Efficiency

To test the putative role of the 5′ UTR of the MDR1 mRNA, we have used the K562 and K562/Adr cell lines. We have used these cell lines for several reasons. First, the short 5′ UTR sequence present in the HT-29 and HT-29/M6 cell lines is identical to the 5′UTR short sequence present in the K562 wild-type cell line (data submitted online). Second, the long 5′UTR that appears in the K562/Adr MDR1 mRNA is identical in sequence to the long 5′UTR MDR1 mRNA that has been reported in the MCF-7/Adr cell line. Third, as previously reported in breast cancer tissues (24), an alternative long 5′UTR appears by alternative splicing in K562/Adr. This 5′UTR lacks 147 bp of the long 5′UTR in K562/Adr and constitutes a quite interesting tool for further studies because it is equivalent to a deletion mutant of the long 5′UTR (Supplementary Fig. S4C). Finally, we have a complete series of K562 cellular sublines that have been made resistant to daunomycin by selective pressure with this drug and constitutes a dynamic model of chemoresistance acquisition. Using the K562-K562/Adr cellular model, we have found that the MDR1 mRNA half-life depends on the 5′UTR present in the MDR1 mRNA. As shown in Fig. 8A, the long 5′UTR MDR1 mRNA has a much longer half-life than the short 5′UTR MDR1 mRNA. Interestingly, the half-life of the MDR1 mRNA containing the alternative splicing form of the long 5′UTR that is 147 bp shorter is similar to the half-life of the short 5′UTR MDR1 mRNA, demonstrating that the 5′UTR sequence is responsible for the differences observed in the half-life between those MDR1 mRNAs.

We have also shown that the half-life of the MDR1 mRNA is regulated by the 5′UTR in the colon carcinoma cell lines, HT-29 and HCT-15 (HCT-15 cells express a Pgp protein translated from a 5′UTR MDR1 mRNA that is similar to the one present in MCF-7/Adr cells; sequence data are submitted as Supplementary Fig. S4A). We have found that the half-life of the MDR1 mRNA in HT-29 cells is shorter than the half-life of the MDR1 mRNA in HCT-15 cells, as shown in Table 1. Besides the long 5′UTR form, HCT-15 cells also express a 147-bp shorter alternative splicing form. As in K562/Adr cells, the half-life of this splicing form is shorter than the half-life of the long 5′UTR MDR1 mRNA (Table 1).

When the secondary structure of the different MDR1 mRNAs was studied using a program software (Vienna RNA

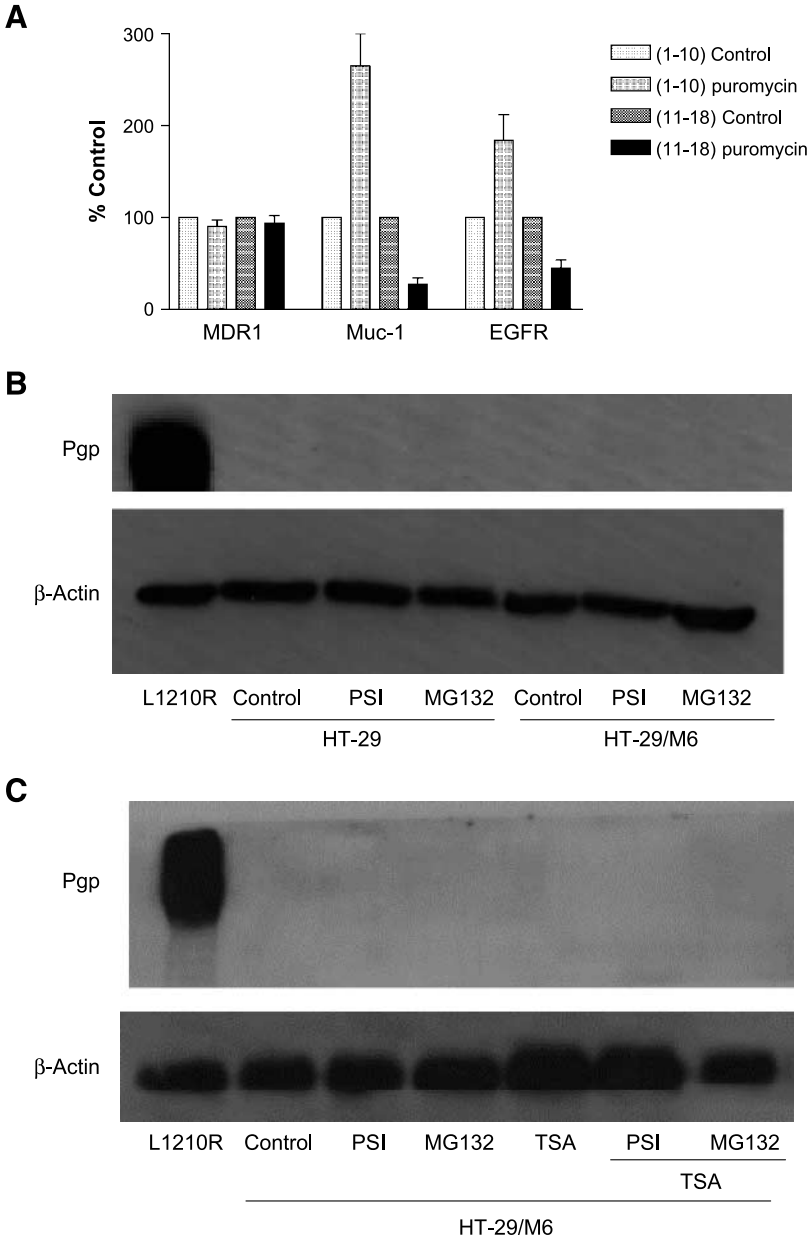

FIGURE 5. Effect of puromycin treatment on the polysome profile distribution of MDR1, Muc-1, and EGFR mRNAs in HT-29/M6 cells. **A.** HT-29/M6 cells were treated with puromycin as described in Materials and Methods, and the polysome profiles distribution of MDR1, Muc-1, and EGFR were determined. Fractions were pooled into two groups. Peak 1 corresponds to a pool of fractions 1 to 10 and represents mostly the monosomes. Peak 2 corresponds to a pool of fractions 11 to 20 and represents mostly active polysomes as shown in Fig. 4A and B. Columns, mean of at least three independent experiments; bars, SD. **B.** Western blot analysis of Pgp expression in HT-29 and HT-29/M6 cells treated or not with PSI or MG-132 (proteasome inhibitors) for 24 h. The L1210R cell line is included as a positive control. Lane 1, L1210R. Lane 2, HT-29. Lanes 3 and 4, HT-29 treated with PSI and MG-132, respectively. *Lane 5,* HT-29/M6 control. Lanes 6 and 7, HT-29/M6 treated with PSI and MG-132, respectively. As a loading control, β-actin in each sample is presented. **C.** Western blot analysis of Pgp expression in HT-29/M6 cells treated or not with TSA, PSI, and MG-132 alone or in combination for 24 h. The L1210R cell line is included as a positive control. Lane 1, L1210R. Lane 2, HT-29/M6. Lanes 3 and 4, HT-29/M6 treated with PSI and MG-132, respectively. Lane 5, HT-29/M6 TSA. Lanes 6 and 7, HT-29/M6 treated with PSI and MG-132 in the presence of TSA, respectively. As a loading control, β-actin in each sample is presented.

package[3]), significant differences between the complete long 5′UTR MDR1 mRNA and the 147-bp-deleted long 5′UTR MDR1 mRNA were found, suggesting that the differences in MDR1 mRNA half-lives may be related to a double stem loop that is missing in the alternative splicing form of this mRNA as shown in Fig. 8B.

Finally, the relationship between the expression of the long 5′UTR MDR1 mRNA and the final expression of the Pgp protein was clearly established using a set of K562 cell lines that were made resistant to increasing concentrations of daunomycin by selective pressure with this drug. As shown in Fig. 9A-C, increasing concentrations of daunomycin were able to produce an increase in the expression of MDR1 mRNA levels. At low concentrations of daunomycin (nmol/L; d10 and d15), the MDR1 mRNA expressed by the cells was mostly the short 5′UTR MDR1 mRNA present in the K562 wild-type and in the HT-29 and HT-29/M6 cell lines. However, at higher doses of daunomycin (d20 and further), the two different forms of the long 5′UTR MDR1 mRNA are expressed. When the presence of the functional Pgp protein expression was determined in K562 cells by daunomycin accumulation experiments, a functional Pgp protein was only found in d20 and resistant cellular sublines to higher daunomycin concentrations as shown in Fig. 9C. These results show a good correlation between the expression of functional active Pgp protein and the increase in the activity of the upstream

[3] http://www.tbi.univie.ac.at/~ivo/RNA

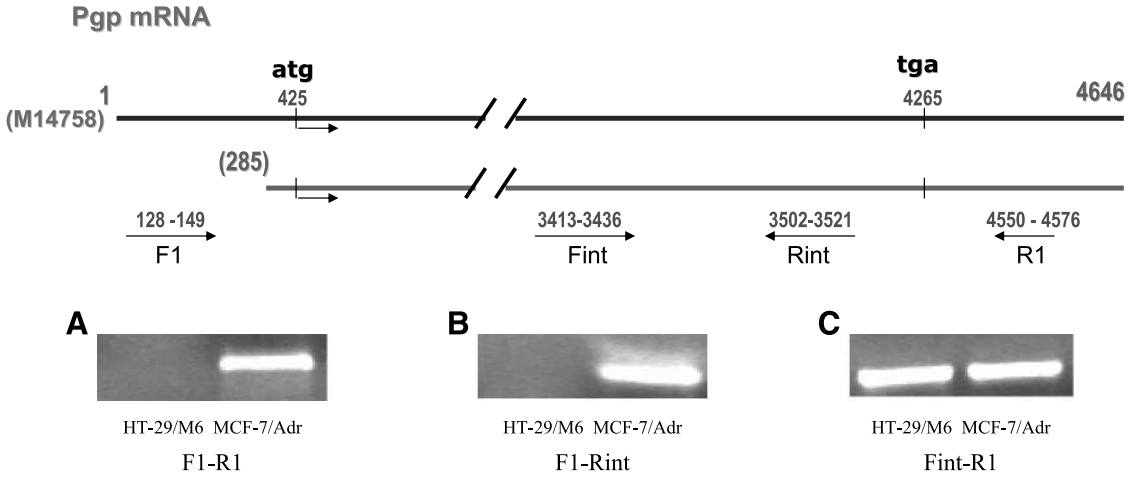

FIGURE 6. Amplification by RT-PCR of different fragments of MDR1 cDNA. **A.** RT-PCR amplification of the complete MDR1 cDNA with the F1 and R1 primers. Lane 1, HT29/M6. Lane 2, MCF-7/Adr. **B.** RT-PCR amplification of the 5′ end of the MDR1 cDNA with the F1 and Rint primers. Lane 1, HT29/M6. Lane 2, MCF-7/Adr. **C.** RT-PCR amplification of the 3′ end of the MDR1 cDNA with the Fint and R1 primers. Lane 1, HT29/M6. Lane 2, MCF-7/Adr.

promoter of the *MDR1* gene, suggesting that the presence of the long 5′UTR in the MDR1 mRNA confers an increased translation efficiency to this mRNA probably due to its longer half-life.

Finally, the relationship between the expression of the long 5′UTR MDR1 mRNA and the final expression of the Pgp protein was also shown, analyzing the distribution of the 5′ UTR MDR1 mRNA and the 147-bp deleted long 5′UTR MDR1 mRNA in polysome profiles from K562/Adr cells as shown in Fig. 10. Only the long 5′UTR MDR1 mRNA was detected in the active polysome fractions as shown in Fig. 10A. The 147-bp deleted long 5′UTR MDR1 mRNA was not found in the K562/Adr polysome profile as shown in Fig. 10B, either by a conventional RT-PCR analysis (Fig. 10B) or by real-time RT-PCR analysis (data not shown), suggesting that the integrity of the long 5′UTR of the MDR1 mRNA is a requirement for efficient translation of the Pgp protein in K562/Adr cells. Furthermore, in HCT-15, a colon carcinoma cell line expressing Pgp and harboring the long 5′UTR MDR1 mRNA, either a siRNA oligonucleotide specific for the long 5′UTR or a siRNA specific for a sequence in exon 14 (common to both MDR1 mRNAs) was able to induce a significant decrease in Pgp protein levels, demonstrating that the mRNA with the long 5′UTR is indeed the form actively translated (Fig. 11).

Discussion

The results presented herein show that the regulation of Pgp expression is a complex process involving transcriptional as well as post-transcriptional events, such as the use of an

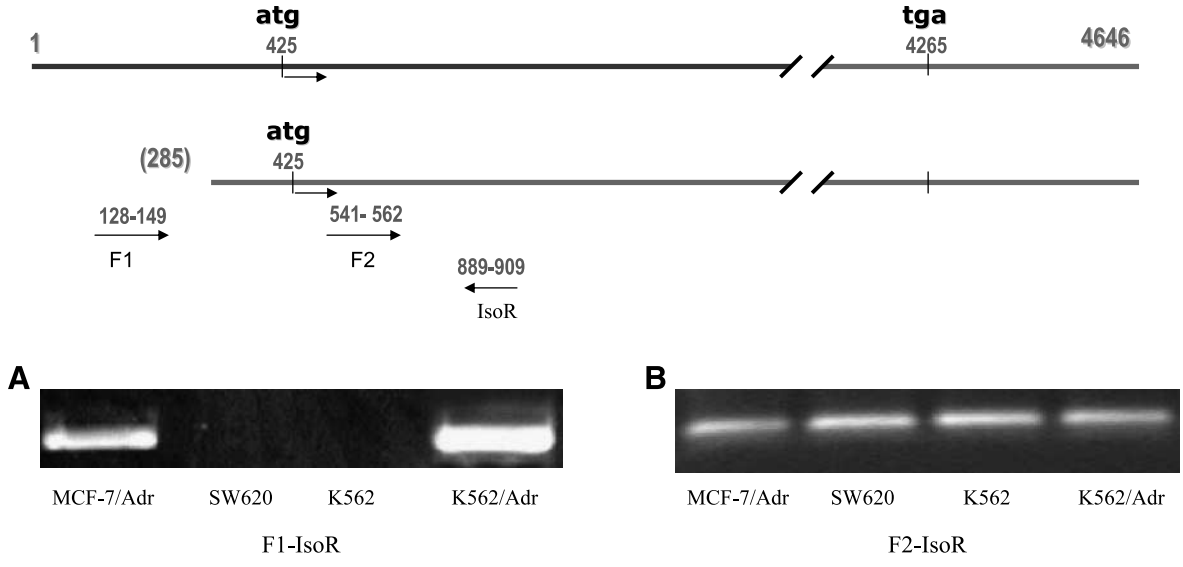

FIGURE 7. Amplification by RT-PCR of the distal and proximal 5′ ends of the MDR1 cDNA. **A.** RT-PCR amplification of the distal 5′ end of the MDR1 cDNA with the F1 and IsoR primers. Lane 1, MCF-7/Adr. Lane 2, SW620. Lane 3, K562. Lane 4, K562/Adr. **B.** RT-PCR amplification of the proximal 5′ end of the MDR1 cDNA with the F2 and IsoR primers. Lane 1, MCF-7/Adr. Lane 2, SW620. Lane 3, K562. Lane 4, K562/Adr.

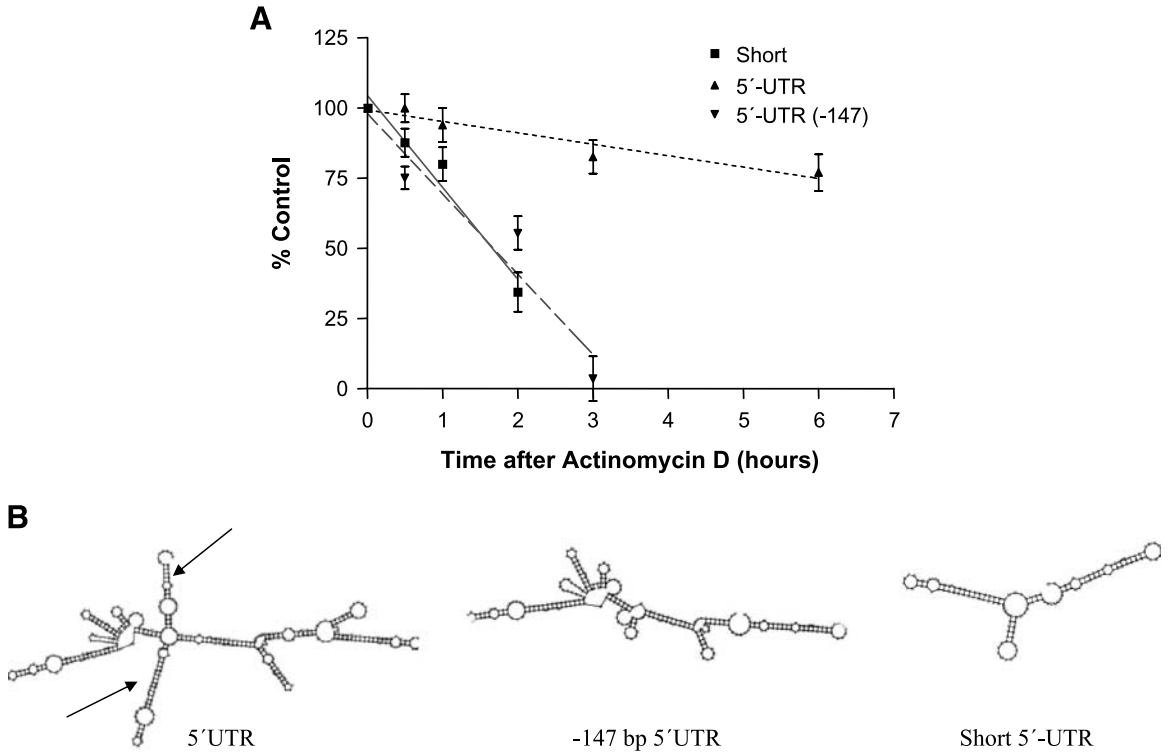

FIGURE 8. MDR1 mRNA half-life. **A.** K562 and K562/Adr cells were treated with 4 μmol/L actinomycin D to block transcription. Total RNA was isolated at different times, and the decay of the 5′ short, long, and the −147 splicing forms of MDR1 mRNA were determined. **B.** Putative secondary structures of the different 5′ UTR MDR1 mRNAs (Vienna RNA package http://www.tbi.univie.ac.at/~ivo/RNA). Black arrows, putative stem loops associated with MDR1 mRNA half-life.

alternative promoter, post-transcriptional destabilization of MDR1 mRNA, and translational blockade of Pgp expression. The key element of the mechanisms of regulation of Pgp expression resides in the 5′UTR of the MDR1 mRNA.

We and others have reported that the iHDACs TSA and SAHA induce two major effects in drug-resistant cells lines: down-regulation of Pgp and apoptosis induction. In that sense, we have shown that TSA markedly reduced Pgp expression in L1210R drug-resistant cells (25) and ''sensitized'' these cells to daunomycin (26, 27), suggesting that iHDACs might have a therapeutic potential against tumors with acquired resistance phenotype. However, Jin and Scotto have reported an increase in the steady-state level of MDR1 mRNA in the human colon carcinoma SW620 cells upon treatment with TSA (17). In the present study, we have shown that there is an increase in MDR1 mRNA not only in SW620 cells but also in HT-29 and HT-29/M6 cells. However, the increase observed in MDR1 mRNA after iHDACs treatment does not parallel an increase either in Pgp protein or in Pgp activity. In that sense, a recently published work shows, in agreement with us, that there is constitutive expression of MDR1 mRNA in HT-29 cells, but no Pgp protein or activity could be detected (23).

Table 1. MDR1 mRNA Half-Life

	Short (min)	5′UTR (min)	5′UTR (−147) (min)
K 562 wt	104 ± 54	ND	ND
K 562 adr	ND	707 ± 202	104 ± 49
HCT-15	ND	864 ± 180	240 ± 125
HT-29	306 ± 67	ND	ND

NOTE: H T-29 and HCT-15 cells were treated with 4 μmol/L actinomycin D to block transcription. Total RNA was isolated at different times, and the decay of the 5′ short, long, and −147 splicing forms of MDR1 mRNA were determined. Estimated half-life of each MDR1 mRNA isoform is presented and compared with the estimated half-lives of the same MDR1 mRNA isoforms present in K562 and K562/Adr cells.
Abbreviation: ND, not determined.

Once that we showed the lack of Pgp expression in these cell lines after iHDACs treatment, we decided to study the putative mechanisms involved in this phenomenon. First, we tried to determine the subcellular distribution of the MDR1 mRNA. We isolated the nuclear and the cytoplasmic RNA and analyzed MDR1 mRNA in both fractions. The results show that iHDACs increased MDR1 mRNA in nuclear as well as in cytoplasmic fractions. Although an important fraction of the MDR1 mRNA remained in the nuclei after TSA treatment, there was an increase of cytoplasmic MDR1 mRNA that should be suitable for translation. For this reason, we studied if, in fact, this mRNA was able to bind to ribosomes, this being the first step for an efficient translation. Our results show that as expected, MDR1 mRNA seemed mostly in the membrane-bound ribosomes, and that after TSA treatment, an increase in MDR1 mRNA levels associated with the membrane-bound ribosomes was observed. Because this increase does not parallel any significant expression of Pgp protein, we conclude that there is a translational blockade of Pgp expression in these cell lines.

A rapid turnover of the Pgp protein as an alternative mechanism for the lack of Pgp was discarded after incubating the cells in the presence of different protease and proteasome inhibitors. As expected, if rapid degradation of Pgp protein was the mechanism responsible for the lack of Pgp protein in these cell lines, none of these treatments resulted in Pgp protein detection.

Translational control is suggested as a possible mechanism due to the abnormal distribution of MDR1 mRNA in the polysome profiles in HT-29/M6 cells, when compared with the distribution of other control mRNAs, such as Muc-1, EGFR, and GAPDH. In addition, the study of the mRNA distribution for Pgp and other genes in polysome profiles done in the presence and absence of puromycin strongly suggests a translational blockade of MDR1 mRNA in HT-29/M6 cells. Our data show the expected results on the distribution of Muc-1 and EGFR after puromycin treatment. However, puromycin had no effect on MDR1 mRNA distribution in the polysomes,

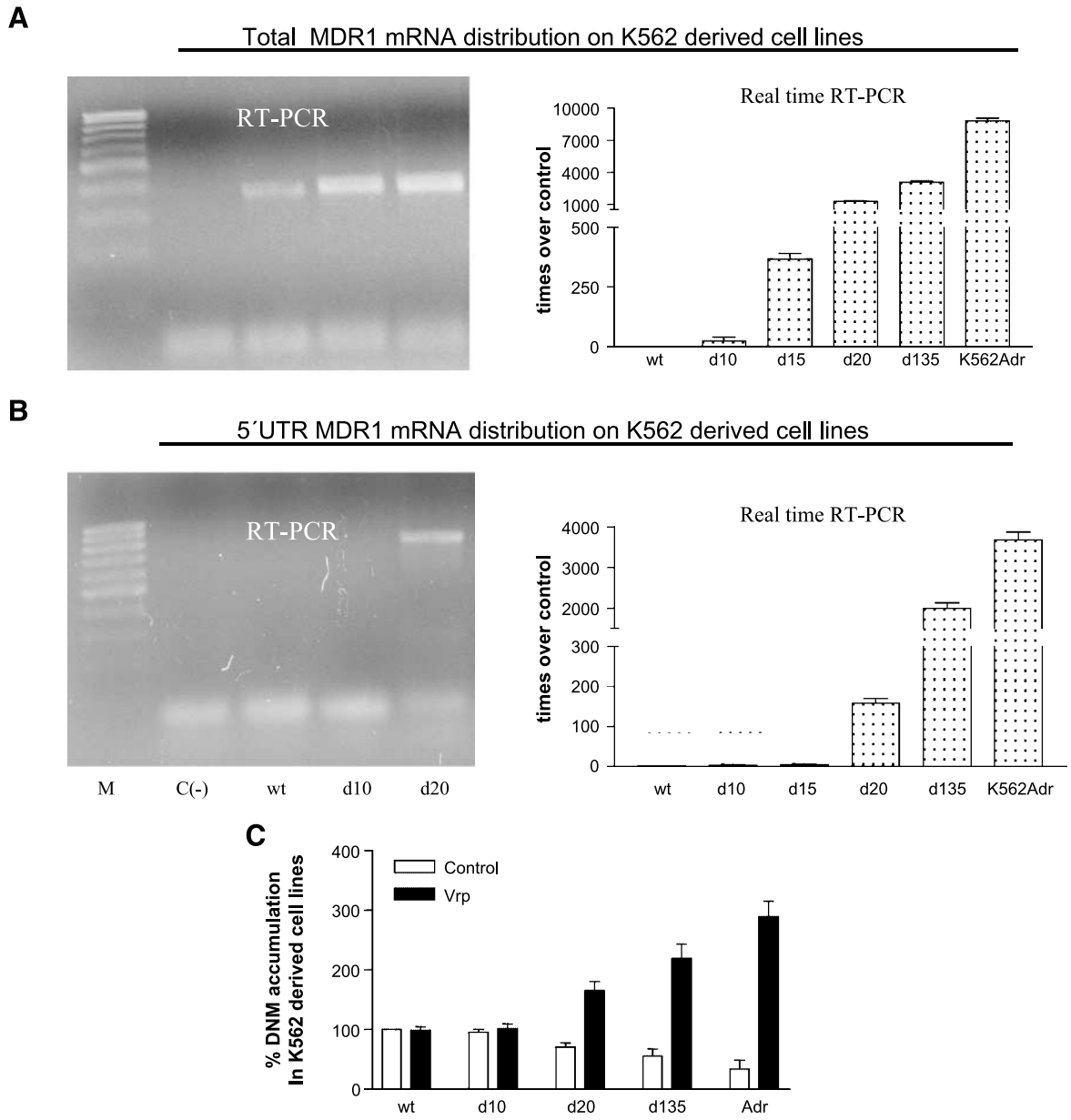

FIGURE 9. Long 5′UTR and Pgp expression. Daunomycin-resistant K562 sub–cell lines were grown as previously described. Total RNA was isolated, and the expression of the different 5′UTR MDR1 mRNAs was determined by RT-PCR. **A.** Left, expression of the total MDR1 mRNA visualized by conventional RT-PCR followed by agarose gel electrophoresis using probes that did not discriminate among the different 5′UTR forms. Right, analysis by real-time RT-PCR of the quantitative expression of the total MDR1 mRNA using the same probes. **B.** Left, expression of the 5′ long UTR MDR1 mRNA in the same cell lines visualized by conventional RT-PCR followed by agarose gel electrophoresis using primers from the 285-bp region. Right, analysis by real-time RT-PCR of the quantitative expression of the 5′ long UTR MDR1 mRNA in the same cell lines using the same primers. **C.** Pgp activity on K65 derived cell lines. Daunomycin accumulation in the presence and absence of verapamil in the daunomycin-resistant K562 cell sub–lines. Columns, means in at least three independent experiments; bars, SD.

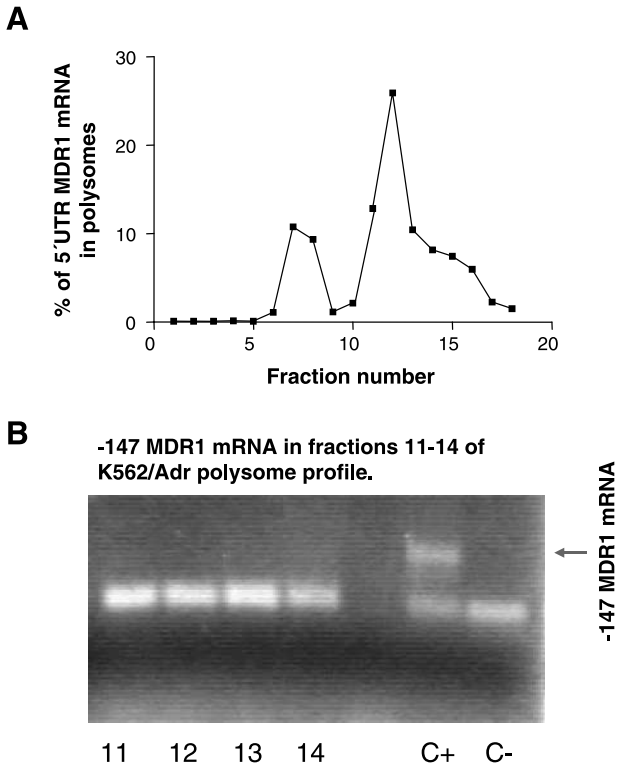

FIGURE 10. K562/Adr polysome profile. **A.** Polysome profile distribution of the 5′ long UTR MDR1 mRNA in K562/Adr cells. **B.** Expression of the −147 splicing form of the MDR1 mRNA in the active polysome fractions visualized by conventional RT-PCR, followed by agarose gel electrophoresis using primers in the splicing site junction to discriminate from the 5′ long UTR MDR1 mRNA.

demonstrating that this mRNA is not being actively translated in these cells. Translational control of Pgp expression has also been shown in K562 cells (28). In this case, the authors did not detect MDR1 mRNA associated with translationally active polysomes. Independently of the polysome distribution of the MDR1 mRNA in K562 and colon carcinoma cell lines, in both cases, there is a complete blockade of the Pgp protein translation.

Next, we wanted to study the regions of the MDR1 mRNA involved in this translational regulation.

To map the region responsible for the translational control of Pgp expression, we initially tried to obtain the cDNA from the MDR1 mRNA. Interestingly, with the set of primers used for the RT-PCR, we were able to obtain the complete MDR1 cDNA in MCF-7/Adr cells, but we could not obtain MDR1 cDNA in HT-29, HT-29/M6, and SW620 cells. To further study the reasons of this result, a second set of primers was designed in the coding sequence. The cDNA corresponding to the 3′ end of the MDR1 mRNA was obtained in HT-29, HT-29/M6, and SW620 cells, as well as in MCF-7/Adr cells. On the contrary, the 5′ end cDNA was only obtained in the MCF-7/Adr cell line, suggesting that the 5′ end of the MDR1 mRNA shows some differences in MCF-7/Adr cells when compared with HT-29 and HT-29/M6 colon cancer cells. We designed different sets of primers covering the whole 5′ end of the MDR1 mRNA at 400-bp intervals. All the primers were able to amplify MDR1 mRNA in MCF-7/Adr, HT-29, and HT-29/M6 cells, except for the very first primer corresponding to the first 400 bp at the 5′ end of the MDR1 mRNA. Using these primers, we could amplify the corresponding fragment in MCF-7/Adr and K562/Adr cells, but not in HT-29, HT-29/M6, and K562 cells. Our data suggest that the translational blockade of MDR1 mRNA in colon carcinoma cell lines and in K562 cells could be overcome by alterations in the 5′ end of the MDR1 mRNA in the resistant variant of these cell lines. The origin and nature of these alterations could be elucidated when the amplified bands were sequenced. In fact, Raguz et al. (24) have reported the activation of a *MDR1* upstream promoter in breast carcinoma samples. Interestingly, the authors used MCF-7/Adr and K562/Adr cells as control, and in both cases, they showed a preferential use of the upstream *MDR1* promoter, whereas the active promoter in the parental MCF-7 and K562 cells was the downstream promoter. Both promoters were able to translate the same protein because they used the same ATG codon, but the mRNA transcribed from the upstream promoter was ~285 bp longer in its 5′ end than the MDR1 mRNA from the downstream promoter. Because the primers that we designed to cover the first 400 bp of the 5′ end mapped inside of these 285 bp, we could only detect the MDR1 mRNA transcribed from the upstream promoter. Our data, together with the data in the literature, strongly suggest that expression of MDR1 mRNA is necessary but not sufficient for Pgp protein expression, indicating that MDR1 mRNA is subjected to a negative translational control. We hypothesize that during the acquisition of chemoresistance, there is a switch from the downstream to the upstream *mdr1* promoter, and this promoter produces a MDR1 mRNA that is more efficiently translated, being the correlation between the promoter used and the efficiency of Pgp translation, the most important findings reported in this article.

The role of the longer MDR1 mRNA is not completely understood. However, Yague et al. (28) have shown that the half-life of the MDR1 mRNA in the K562/Adr cell line is

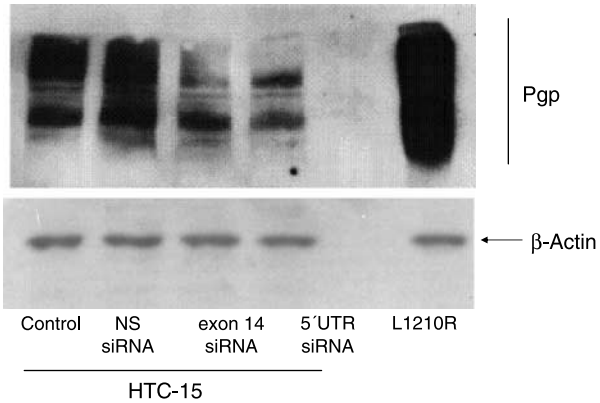

FIGURE 11. siRNA directed toward 5′UTR MDR1 mRNA effect on Pgp expression in HTC-15 cells. HTC-15 cells were plated and transfected with three different siRNAs oligonucleotides (30 nmol/L; Ambion, Inc.). A nonspecific siRNA (*NS*), a validated siRNA targeted to a Pgp sequence in exon 14 (*exon 14*), and an siRNA designed and targeted to the differentially expressed 5′UTR of Pgp (*5′UTR*) 48 h after transfection Pgp levels were determined by Western blot.

longer than in the K562 cell line, a result that has been corroborated in our laboratory (Fig. 8A). The authors do not discriminate between the two different MDR1 mRNA transcribed from the upstream or the downstream promoter. However, we have been able to do it, and we can conclude that the use of the upstream *mdr1* promoter with the additional 285-bp 5′ end leads to an increase in the half-life of the MDR1 mRNA, as compared with the shorter downstream *mdr1* promoter. Furthermore, determining the half-life of the alternative splicing form of the long 5′UTR MDR1 mRNA, we have shown that the increase in the MDR1 mRNA half-life may be related to two stem loops located in the 5′UTR of the upstream promoter. Furthermore, the differences in the half-life of the 5′UTR MDR1 mRNA take place also in HT-29 and HCT-15 colon carcinoma cells. The increase in the MDR1 mRNA expression levels as a consequence of its stabilization could improve the ratio of the translated Pgp. However, a direct effect of the longer 5′ end in the translation efficiency is also plausible. In this sense, we have shown that the expression of an active Pgp protein correlates with the activation of the upstream promoter of the *mdr1* gene in several K562 cellular sublines obtained by selective pressure with increasing concentrations of daunomycin.

The key role of the 5′UTR in translation efficiency of Pgp protein has also been shown in HCT-15 colon cancer cells transfected with two different siRNAs, one of them specifically targeted to the 5′UTR differentially expressed region, and the other one targeted to a sequence in exon 14 of the MDR1 mRNA. In both cases, we could detect a significant decrease in Pgp protein expression, demonstrating that the 5′ long UTR form is actually the mRNA translated in the ribosomes.

Finally, translational control mediated by 5′UTR of specific mRNAs is not an uncommon feature in nature. For instance, thymidylate synthase shows a polymorphic 5′UTR containing two or three tandem repeats, and a recent work has shown that the thymidylate synthase mRNA with three tandem repeats is translated more efficiently than the mRNA with two tandem repeats (29). Therefore, we can conclude that UTRs may have a profound effect on the regulation of expression of specific mRNAs.

Materials and Methods

Cell Lines and Culture

HT-29, HT-29/M6 (methotrexate-resistant subline derived from HT-29), and SW620 human colon carcinoma cell lines were kindly donated by Dr. Francisco X. Real (IMIM, Barcelona, Spain). MCF-7/Adr (Adriamycin-resistant subline derived from MCF-7) human breast carcinoma cell line was kindly donated by the Vincent T. Lombardi Cancer Center (Georgetown University, Washington D.C.). HTC-15 colon carcinoma cell line was purchased from the American Type Culture Collection (LGC Promochem). Cells were grown at 37°C in 5% CO_2, with DMEM (Life Technologies BRL Invitrogen) supplemented with 10% fetal calf serum (Bio Whittaker), 2 mmol/L L-glutamine (Life Technologies BRL Invitrogen), 1 mmol/L sodium pyruvate (Life Technologies BRL Invitrogen), 50 units/mL penicillin, and 50 μg/mL streptomycin (Life Technologies BRL Invitrogen). The murine leukemia cell lines L1210, L1210R (daunomycin-resistant subline derived from L1210), K562 (a human erythroleukemia cell line), and K562/Adr (Adriamycin-resistant subline derived from K562) were grown as previously described (25).

Flow-Cytometric Analysis of Cell Cycle Distribution

HT-29, HT-29/M6, and SW620 human colon carcinoma cell lines were incubated with TSA at selected times up to 24 h. After harvesting the cells, 1×10^6 cells were centrifuged and washed with cold 10 mmol/L phosphate buffer (pH 7.4), supplemented with 2.7 mmol/L KCl and 137 mmol/L NaCl (PBS) and centrifuged again. The pelleted cells were resuspended in 75% cold ethanol, fixed for 1 h at −20°C, centrifuged, and resuspended in 0.5 mL of PBS supplemented with 0.5% Triton X-100 and 0.05% RNase A. Then, cells were incubated for 30 min at room temperature, stained with propidium iodide, and the distribution of cellular DNA content was analyzed by flow cytometry in an Epics XL flow cytometer (Beckman Coulter Co.). Nonviable cells were excluded from the analysis on the basis of their abnormal size.

Western Blot

Treated or untreated HT-29 and HT-29/M6 cells were washed twice with PBS scraped, centrifuged, and lysed in a buffer containing 150 nmol/L NaCl, 1% NP40, 0.5% sodium deoxycholate, 0.1% SDS, 50 nmol/L Tris (pH 8) and proteases and phosphatase inhibitors. L1210R cells grown in suspension were washed twice with PBS and incubated with lysis buffer. Protein determinations were done by the Bradford method (Bio-Rad). Determination of Pgp expression was done using the monoclonal antibody (mAb) C-219 (Centocor Inc.) as previously described (30, 31), followed by enhanced chemiluminescence (Amersham International) to develop protein bands.

Drug Accumulation Studies

Steady-state intracellular accumulation assays of the fluorescent daunomycin in the absence or in the presence of verapamil were done as previously described (32). Pgp activity was also determined using the Vybrant Multidrug Resistance Assay Kit (V-13180) from Molecular Probes following the manufacturer's instructions. Samples were analyzed in a fluorescence reader (Fluostar Galaxy) to determine intracellular calcein accumulation.

Real-time RT-PCR

Total RNA from nontreated or TSA-treated cells was isolated using the TRI reagent (Sigma-Aldrich, Co.) or the RNeasy Mini Kit (Qiagen GmbH). To eliminate potential DNA contamination, total RNA was treated with RQ1 DNase (Promega Corp.) for 30 min at 37°C, followed by 2 min at 94°C. Reverse transcription of 1 μg RNA was done using the TaqMan Reverse Transcription Reagents kit (Applied Biosystems) according to the manufacturer's instructions. Real-time quantitative PCR was done to amplify 20 ng of cDNA using the ABI Prism 7700 Sequence Detector System (Applied Biosystems). Primers and probe to amplify Pgp were designed using the Primer Express software (Applied Biosystems).

The sequences of the primers for MDR1 were PgpF (sense) 5′-gactatgccaaagccaaaatat-3′ and PgpR (antisense) 5′-cttccaa-tgtgttcggcattag-3′. The sequence of the TaqMan probe for MDR1 was 5′-aaaaaaccccttttgattgacagctacagcac-3′. Pgp TaqMan probes were labeled with 6-FAM in the 5′ end as the reporter dye, and with TAMRA in the 3′ end as the quencher dye. GAPDH was used as an endogenous reference in multiplex PCR. GAPDH TaqMan probe was labeled with VIC in the 5′ end as the reporter dye, and with TAMRA in the 3′ end as the quencher dye. MDR1 mRNA relative gene expression was calculated by the comparative Ct method referred to the GAPDH housekeeping gene expression (ABI Prism 7700 Sequence Detection System: User Bulletin 2, Applied Biosystems).

RT-PCR Analysis of the MDR1 mRNA

Total RNA from different cell lines was isolated after treatment with RQ1 DNase and reverse transcribed as described above. The cDNAs obtained were amplified by PCR using the appropriate set of primers. The primer sequences were F1 (cctcctggaaattcaacctgtttcgc), R1 (cttttagcaaggcagtcagttacagtc), Fint (gactatgccaaaatatca), Rint (cttccaatgtgttcggcattag), F2 (gtttcgctattcaaattggctt), and ISO (cagcctatctcctgtcgcatt).

The cDNAs were amplified by PCR as follows: 2 min at 94°C and then 40 cycles of 30 s at 94°C, 30 s at 55 to 61°C (depending on the set of primers), 45 s to 2 min (depending on the length of the amplified segment) at 72°C, and 7 min at 72°C. PCR products were resolved by electrophoresis on 0.5% to 2% (w/v) agarose gels. Bands were visualized with ethidium bromide.

Isolation of Nuclear and Cytoplasmic RNA

Control or TSA-treated cells were centrifuged in cold PBS for 5 min at 500 × *g*, and the cellular pellet was vortexed (at half potency) 5 s. Then, 2.0 mL of NP40 lysis buffer [10 mmol/L Tris-HCl (pH 7.4), 10 mmol/L NaCl, 3 mmol/L $MgCl_2$, 0.5% NP40] were added while vortexing. Cells were incubated 5 min on ice and centrifuged at 500 × *g* for 5 min at 4°C. The supernatant containing the cytoplasmic fraction and the pellet containing the nuclei were frozen at −80°C. RNA from each fraction was isolated using the RNeasy Mini Kit (Qiagen GmbH) according to the manufacturer's instructions.

Isolation of Free Polysomes and Membrane-Bound Polysomes

Control or TSA-treated cells were resuspended in a hypotonic buffer [10 mmol/L KCl, 1.5 mmol/L $MgCl_2$, 10 mmol/L Tris-HCl (pH 7.4)] and homogenized with 10 strokes in a Dounce homogenizer. The homogenate was diluted (5:1) in a sucrose buffer [2.5 mol/L sucrose, 0.15 mol/L KCl, 5 mmol/L $MgCl_2$, 50 mmol/L Tris-HCl (pH 7.4)]. The mixture was layered on two volumes of the same buffer. Three volumes of 2.05 mol/L sucrose buffer were then added on top of the 2.5 mol/L sucrose buffer, and one volume of 1.2 mol/L sucrose buffer was then added on top of the 2.05 mol/L sucrose buffer. The mixture was centrifuged at 82,000 × *g* for 5 h at 4°C. Fractions were collected and frozen at −80°C for subsequent RNA extraction.

Polysome Profiles

Control or TSA-treated cells were treated before harvesting (20 min) with 40 μg/mL cycloheximide to prevent runoff of ribosomes. Cells were then centrifuged in PBS, and the cellular pellet was resuspended in 1 mL of homogenization buffer [0.2 mol/L sucrose, 0.2 mol/L Tris-HCl (pH, 8.5), 35 mmol/L $MgCl_2$, 10 mmol/L EDTA, 25 mmol/L EGTA, 0.1 mol/L KCl, 4 μg/mL polyvinylsulfate, 0.5% NP40, 10 μg/mL cycloheximide, 80 units of RNasin/mL, 1% Triton X-100] and homogenized with 10 strokes in a Dounce homogenizer. The homogenate was centrifuged at 10,000 × *g* for 20 min at 4°C, and the supernatant was layered on a sucrose gradient (15-40%) containing 100 mmol/L KCl, 20 mmol/L $MgCl_2$, and 10 mmol/L EGTA. The gradient was centrifuged at 133,000 × *g* for 4 h at 4°C. After centrifugation, 0.5-mL fractions were collected, top to bottom, and frozen at −80°C for subsequent RNA extraction using the RNeasy Mini Kit (Qiagen GmbH) according to the manufacturer's protocol.

Determination of MDR1 mRNA Half-life

K562, K562/Adr, HTC-15, and HT-29 cell lines were treated with 4 μmol/L actinomycin D to block transcription. RNA was isolated as previously described at different times after treatment, and the different 5′ UTR MDR1 mRNAs decay was determined by real-time RT-PCR.

Small Interfering RNA–Mediated Decrease of Pgp Protein Translation

HCT-15 colon cancer cells were plated in normal medium without antibiotic and transfected with two different small interfering RNAs (siRNA) oligonucleotides (30 nmol/L; Ambion, Inc.). The validated siRNA (Ambion, Inc.) targeted to a Pgp sequence in exon 14 does not discriminate between MDR1 mRNAs produced by the upstream or downstream *mdr1* promoters, whereas the second siRNA was predesigned and targeted to the differentially expressed 5′UTR of Pgp (produced only by the upstream *mdr1* promoter). Transfection was done with Lipofectamine (Invitrogen Corporation) in siRNA transfection medium (Santa Cruz Biotechnology Inc.) according to the manufacturer's instructions. Transfection medium was removed after 7 h, and cells were cultured in normal medium for 48 h. Pgp protein and MDR1 mRNA levels were determined by Western blot and real-time RT-PCR, respectively. The siRNAs sequences were as follows:

validated siRNA: sense GGAUAUUAGGACCAUAAAUtt;
antisense AUUUAUGGUCCUAAUAUCCtg
predesigned siRNA: sense GGUAUCUGUUUAACAUUUCtt;
antisense GAAAUGUUAAACAGAUACCtc

References

1. Gottesman MM. Mechanisms of cancer drug resistance. Annu Rev Med 2002; 53:615–27.

2. Ambudkar SV, Dey SHCA, Ramachandra M, Pastan I, Gottesman MM. Biochemical, cellular, and pharmacological aspects of the multidrug transporter. Annu Rev Pharmacol Toxicol 1999;39:361–98.

3. Gottesman MM, Fojo T, Bates SE. Multidrug resistance in cancer: role of ATP-dependent transporters. Nat Rev Cancer 2002;2:48–58.

4. Tan B, Piwnica-Worms D, Ratner L. Multidrug resistance transporters and modulation. Curr Opin Oncol 2000;12:450–8.

5. Johnstone RW, Ruefli AA, Smyth MJ. Multiple physiological functions for multidrug transporter P-glycoprotein? Trends Biochem Sci 2000;25:1–6.

6. Johnstone RW, Ruefli AA, Tainton KM, Smyth MJ. A role for P-glycoprotein in regulating cell death. Leuk Lymphoma 2000;38:1–11.

7. Dean M, Rzhetsky A, Allikmets R. The human ATP-binding cassette (ABC) transporter superfamily. Genome Res 2001;11:1156–66.

8. Hu Z, Jin S, Scotto KW. Transcriptional activation of the MDR1 gene by UV irradiation. Role of NF-Y and Sp1. J Biol Chem 2000;275:2979–85.

9. Schondorf T, Kurbacher CM, Gohring UJ, et al. Induction of MDR1-gene expression by antineoplastic agents in ovarian cancer cell lines. Anticancer Res 2002;22:2199–203.

10. Vilaboa NE, Galan A, Troyano A, de Blas E, Aller P. Regulation of multidrug resistance 1 (MDR1)/P-glycoprotein gene expression and activity by heat-shock transcription factor 1 (HSF1). J Biol Chem 2000;275:24970–6.

11. Ziemann C, Burkle A, Kahl GF, Hirsch-Ernst KI. Reactive oxygen species participate in mdr1b mRNA and P-glycoprotein overexpression in primary rat hepatocyte cultures. Carcinogenesis 1999;20:407–14.

12. Chen GK, Sale S, Tan T, Ermoian RP, Sikic BI. CCAAT/enhancer-binding protein β (nuclear factor for interleukin 6) transactivates the human MDR1 gene by interaction with an inverted CCAAT box in human cancer cells. Mol Pharmacol 2004;65:906–16.

13. Kuwano M, Uchiumi T, Hayakawa H, et al. The basic and clinical implications of ABC transporters, Y-box–binding protein-1 (YB-1) and angiogenesis-related factors in human malignancies. Cancer Sci 2003;94:9–14.

14. Ohga T, Uchiumi T, Makino Y, et al. Direct involvement of the Y-box binding protein YB-1 in genotoxic stress-induced activation of the human multidrug resistance 1 gene. J Biol Chem 1998;273:5997–6000.

15. Strauss BE, Shivakumar C, Deb SP, Deb S, Haas M. The MDR1 downstream promoter contains sequence-specific binding sites for wild-type p53. Biochem Biophys Res Commun 1995;217:825–31.

16. Strauss BE, Haas M. The region 3′ to the major transcriptional start site of the MDR1 downstream promoter mediates activation by a subset of mutant P53 proteins. Biochem Biophys Res Commun 1995;217:333–40.

17. Jin S, Scotto KW. Transcriptional regulation of the MDR1 gene by histone acetyltransferase and deacetylase is mediated by NF-Y. Mol Cell Biol 1998;18:4377–84.

18. He LZ, Tolentino T, Grayson P, et al. Histone deacetylase inhibitors induce remission in transgenic models of therapy-resistant acute promyelocytic leukemia. J Clin Invest 2001;108:1321–30.

19. Yuan Y, Zhang J, Scanlon KJ, Lu Z, Qi G. Reversion of multidrug resistance in the P-glycoprotein positive breast cancer cell line (MCF-7/ADR) by introduction of hammerhead ribozyme. Chin Med Sci J 1998;13:24–8.

20. Budworth J, Gant TW, Gescher A. Co-ordinate loss of protein kinase C and multidrug resistance gene expression in revertant MCF-7/Adr breast carcinoma cells. Br J Cancer 1997;75:1330–5.

21. Ogretmen B, Safa AR. Negative regulation of MDR1 promoter activity in MCF-7, but not in multidrug resistant MCF-7/Adr, cells by cross-coupled NF-κB/p65 and c-Fos transcription factors and their interaction with the CAAT region. Biochemistry 1999;38:2189–99.

22. Sharma D, Southworth DR, Green R. EF-G–independent reactivity of a pre-translocation-state ribosome complex with the aminoacyl tRNA substrate puromycin supports an intermediate (hybrid) state of tRNA binding. RNA 2004;10:102–13.

23. Rimet O, Mirrione A, Barra Y. Multidrug-resistant phenotype influences the differentiation of a human colon carcinoma cell line. Biochem Biophys Res Commun 1999;259:43–9.

24. Raguz S, Tamburo DB, Tripuraneni G, et al Activation of the MDR1 upstream promoter in breast carcinoma as a surrogate for metastatic invasion. Clin Cancer Res 2004;10:2776–83.

25. Castro-Galache MD, Ferragut JA, Barbera VM, et al. Susceptibility of multidrug resistance tumor cells to apoptosis induction by histone deacetylase inhibitors. Int J Cancer 2003;104:579–86.

26. Garcia-Morales P, Castro-Galache MD, Menendez-Gutierrez MP, Garcia-Poveda E, Ferragut JA, Saceda M. Trichostatin A effects in different drug-resistant tumor cell lines. Av Diabetol 2002;18:175–9.

27. Ruefli AA, Bernhard D, Tainton KM, Kofler R, Smyth MJ, Johnstone RW. Suberoylanilide hydroxamic acid (SAHA) overcomes multidrug resistance and induces cell death in P-glycoprotein–expressing cells. Int J Cancer 2002;99:292–8.

28. Yague E, Armesilla AL, Harrison G, et al. P-glycoprotein (MDR1) expression in leukemic cells is regulated at two distinct steps, mRNA stabilization and translational initiation. J Biol Chem 2003;278:10344–52.

29. Kawakami K, Salonga D, Park JM, et al. Different lengths of a polymorphic repeat sequence in the thymidylate synthase gene affect translational efficiency but not its gene expression. Clin Cancer Res 2001;7:4096–101.

30. Aleu J, Ivorra I, Lejarreta M, Gonzalez-Ros JM, Morales A, Ferragut JA. Functional incorporation of P-glycoprotein into *Xenopus* oocyte plasma membrane fails to elicit a swelling-evoked conductance. Biochem Biophys Res Commun 1997;237:407–12.

31. Soto F, Planells-Cases R, Canaves JM, et al. Possible coexistence of two independent mechanisms contributing to anthracycline resistance in leukaemia P388 cells. Eur J Cancer 1993;29:2144–50.

32. Soto F, Canaves JM, Gonzalez-Ros JM, Ferragut JA. Rapid kinetics of the interaction between daunomycin and drug-sensitive or drug-resistant P388 leukemia cells. FEBS Lett 1992;301:119–23.